INTERNATIONAL JOURNAL OF GREEN ENERGY
2016, VOL. 13, NO. 4, 352–365
http://dx.doi.org/10.1080/15435075.2014.952426

Taylor & Francis
Taylor & Francis Group

Wind energy potential assessment and techno-economic performance of wind turbines in coastal sites of Buenos Aires province, Argentina

Sibila A. Genchi[a], Alejandro J. Vitale[a,b], M. Cintia Piccolo[a,c], and Gerardo M. E. Perillo[a,d]

[a]Instituto Argentino de Oceanografía (IADO)-Consejo Nacional de Investigaciones Científicas y Técnicas (CONICET), Bahía Blanca, Argentina; [b]Departamento de Ingeniería Eléctrica y de Computadoras, Universidad Nacional del Sur (UNS), Bahía Blanca, Argentina; [c]Departamento de Geografía y Turismo, Universidad Nacional del Sur (UNS), Bahía Blanca, Argentina; [d]Departamento de Geología, Universidad Nacional del Sur (UNS), Bahía Blanca, Argentina.

ABSTRACT

An assessment of wind energy potential was carried out in five sites (four onshore and one offshore) in South-West (SW) of Buenos Aires province (Argentina). We use high-resolution wind data (2 and 5 min) for the period 2009–2012. The power law was used to estimate the wind speed at 30, 40, and 60 m height from the anemometer position. Turbulence intensity and wind direction were analyzed. Statistical analyses were conducted using two-parameter Weibull distribution. A techno-economic analysis based on a set of commercial wind turbines was performed in those sites. The results derived from this work indicate that the SW of Buenos Aires province represents a promising area for the wind energy extraction, which would encourage the construction of wind farms for electricity generation.

KEYWORDS

Argentina; capacity; techno-economic analysis; two-parameter Weibull distribution; wind energy output; wind speed

Introduction

The global increase in energy demand and the rising fossil fuel prices led countries to focus on lower energy consumption and exploit renewable energy sources. The wind is a renewable, inexhaustible, and clean energy source. The wind industry started as a niche business aimed at increasing environmental awareness, but in the past years, it has established itself as the most competitive kind of renewable energy (Molenaar 2003). The recent growth rate of global wind industry has been about 26% (Andrawus et al. 2006). This trend has been driven by developed countries, especially European ones (Recalde 2010). In contrast, wind potential in some world regions, such as the Southeast Asian countries and Latin America, is lightly exploited. This can be due to several factors including, among others, the lack of precise studies concerning wind assessment and the use of limited strategies for its utilization (Karamanis 2013).

Some authors believe that Argentina has a huge wind potential, enabling it to generate electricity and hydrogen. In particular, the greatest wind energy potential is found in the Patagonian region; but, considering Argentina's wind speed map computed at 50 m above ground level (developed by the Wind Energy Regional Center—CREE—and the Ministry of Federal Planning, Public Investment and Services), there are a number of other regions with annual mean values of wind speed that reach 7–8 m s^{-1}, such as the South of Buenos Aires province. In fact, according to the global wind map generated by 3TIER, this area was identified as one of the most important in the world.

There has been a long tradition of wind energy development in Argentina, but it has only received increasing attention over the last two decades. There are few large-scale wind farms operating at high wind speeds, which are located in the Patagonian provinces of Chubut and Santa Cruz, and in the Andean province of La Rioja. At present, small- and medium-scale wind farms are more widespread, although their development has strongly depended on the economic and political conditions of the country. Law 26,190, passed in 2006, establishes the national promotion for the use of renewable energy sources, setting that 8% of the electric power supply should be generated from diverse renewable sources by 2016. Of this percentage, 50% should come from the wind.

Unlike other non-conventional energy sources (e.g., tidal, solar), the wind has a more variable and diffuse energy flux (Weisser 2003). Wind speed and its distribution have an important influence on the performance of a wind turbine (Ayodele et al. 2012). For this reason, the wind has been deeply studied in several world regions (e.g., Archer and Jacobson 2003; Weisser 2003; Bagiorgas, Mihalakakou, and Matthopoulos 2008; Türk Toğrul and İmaş Kizi 2008; Raichle and Carson 2009; Sahin and Bilgili 2009; Diaf and Notton 2013; Onea and Rusu 2013; Gualtieri and Zappitelli 2014). There are few articles focusing on the assessment of wind energy potential in Argentina. For example, in response to a wind farm future settlement, Labraga (1994) carried out a detailed study of the wind characteristics, emphasizing on extreme winds in the central-east Patagonian region. An examination of wind speed power characteristics in the NW of the Patagonia region concluded that the available energy is associated with high gust occurrence, which restricts its exploitation (Palese et al. 2000). Another promising way to use wind as energy source is the production of hydrogen. This has only been done for a site in the Córdoba province (center of Argentina) applying Weibull

CONTACT Sibila A. Genchi genchi.sibila@gmail.com Instituto Argentino de Oceanografía (IADO)-Consejo Nacional de Investigaciones Científicas y Técnicas (CONICET), CC 804, B8000FWB, Bahía Blanca, Argentina.

Color versions of one or more of the figures in the article can be found online at www.tandfonline.com/ljge.

distribution to estimate the annual energy generated by some commercial wind turbines (Rodríguez et al. 2010). Therefore, a feasibility study of the wind as a resource is still insufficient in many regions of Argentina. The aim of this article is to determine the feasibility of wind energy potential in the SW of Buenos Aires province, Argentina. An evaluation of the monthly wind potential at various locations and heights was considered in the current study. Moreover, a techno-economic analysis based on a set of commercial wind turbines was performed.

Study sites and data description

The measurement sites of this study are located in a bay on the SW of Buenos Aires province (Figure 1; Table 1). Four of these sites (General Daniel Cerri, GC; Villa del Mar, VM; Pehuen-Có, PC; and Monte Hermoso, MH) are onshore. The remaining site (oceanographic tower, OT) is offshore, located 20 km away from the nearest coastline. The topographic features of the region are characterized by gently undulating plains. The climate is temperate and sub-humid, with warm summers and cold winters.

The meteorological data (i.e., air temperature, relative humidity, atmospheric pressure, wind direction, and speed) for these stations were recorded during the period 2009–2012, although in some cases data for the full period were not available (Table 1). The data of onshore and offshore stations were sampled over 5 and 2 min intervals, respectively. These shorter time intervals are essential for an accurate assessment of wind characteristics. The onshore stations belong to the Coastal Environmental Monitoring Station (EMAC) network (http://emac.iado-conicet.gob.ar/), which was implemented by researchers from the IADO-CONICET. The offshore station belongs to the Bahía Blanca Port Consortium (CGPBB) and it is installed in a tower structure.

Data analysis procedure

Vertical extrapolation of wind speed data

Wind speed (V) increases with height. Typically, hub height of the small- to medium-scale wind turbines reaches heights of 10 to 60 m above ground. The heights considered in this article were basically 10, 30, and 60 m. The calculation at different heights (h) was carried out applying the power law. The power law exponent (α) was adjusted for each windward face (every 45°) of each site depending on the terrain characteristics, according to Bechrakis and Sparis (2000). Thus, values of power law exponent ranged from 0.10 to 0.35. The equation is given by

$$\frac{V_h}{V_{ref}} = \left(\frac{h}{h_{ref}}\right)^{\alpha}, \tag{1}$$

where V_{ref} is the wind speed measured (m s^{-1}) at the reference height h_{ref} (m) and V_h is the wind speed measured (m s^{-1}) at the height h (m).

Turbulence intensity

The most basic measure of turbulence is the turbulence intensity (TI), which is the ratio between the standard deviation of the wind speed (σ) to the mean wind speed ($\bar{V}$) (Janajreh, Su,

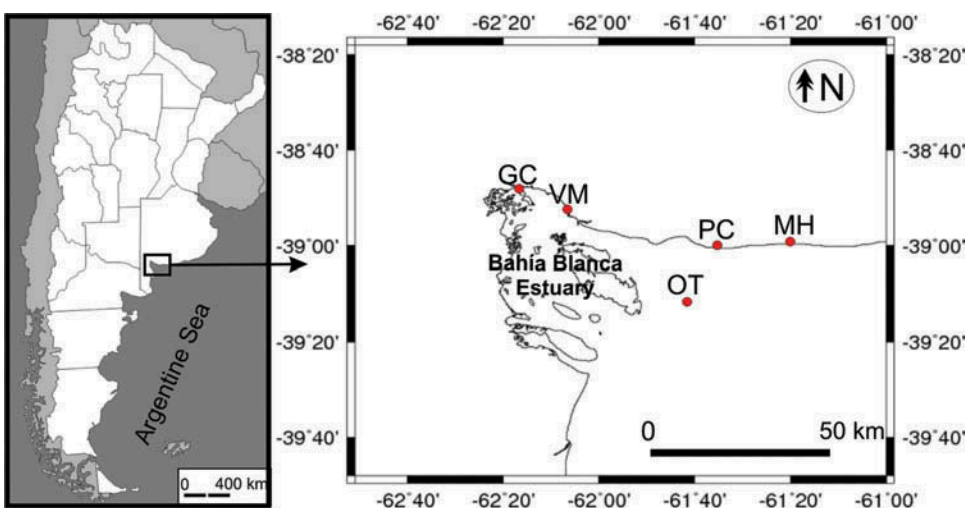

Figure 1. Location map of study sites.

Table 1. Characterization of Study Sites.

Site/Station	Location	Latitude (decimal degree)	Longitude (decimal degree)	Elevation above sea level (m)	Anemometer height (m)	Study Period	Data sampling interval (min)[a]
General Daniel Cerri (GC)	Onshore	−38.75	−62.38	2	10	2009–2012	5
Villa del Mar (VM)	Onshore	−38.85	−62.11	1	10	2009–2011	5
Pehuen Có (PC)	Onshore	−39.00	−61.56	9	13	2009–2012	5
Monte Hermoso (MH)	Onshore	−38.98	−61.31	6	10	2009–2012	5
Oceanographic tower (OT)	Offshore	−39.19	−61.69	–	8	2009–2010	2

[a]The data were further averaged over 10 min for the statistical analysis.

and Alan 2013). The time period is normally lower than an hour (Mirhosseini, Sharifi, and Sedaghat 2011). In this article, turbulence intensity was calculated every 30 min (i), based on the following expression:

$$TI = \frac{\sigma_i}{\bar{V}_i}. \tag{2}$$

According to Olaofe and Folly (2013), values under 0.10 indicate a low turbulence level; a moderate level is approximately equal to 0.25 and values over 0.25 indicate a high level.

Wind speed probability distribution

Wind speed distribution is a key factor in the wind resource evaluation of a given site (Tiang and Ishak 2012). Different theoretical models, such as Weibull, Rayleigh, Lognormal, and Gamma, are applied to fit the distribution of wind speed data. However, several studies (e.g., Ucar and Balo 2009; Kitaneh, Alsamamra, and Aljunaidi 2012; Rehman et al. 2012; Ramos and Iglesias 2014) showed that the Weibull distribution model proved to be the best one due to its great flexibility and simplicity.

The general form of Weibull distribution function for wind speed data is

$$f(V) = \left(\frac{k}{c}\right)\left(\frac{V}{c}\right)^{k-1} \exp\left[-\left(\frac{V}{c}\right)^{k}\right], \tag{3}$$

where $f(V)$ is the probability density function of observed wind speed data, and k (dimensionless) and c (m s^{-1}) are the shape and scale parameters, respectively. There are several methods to calculate k and c such as maximum likelihood, method of moments, standard deviation, and graphical method. The maximum likelihood method is selected because it generally produces lower mean squared errors associated with model parameter estimates for large samples (Morgan et al. 2011; Zhang et al. 2013) as in this study. It is expressed by the followings equations (Stevens and Smulders 1979):

$$k = \left[\frac{\sum_{i=1}^{n} V_i^k ln(V_i)}{\sum_{i=1}^{n} V_i^k} - \frac{\sum_{i=1}^{n} ln(V_i)}{n}\right]^{-1}, \tag{4}$$

where V_i is the wind speed in time step i and n is the number of data points.

$$c = \left[\frac{1}{n}\sum_{i=1}^{n} V_i^k\right]^{1/k}. \tag{5}$$

The most probable and optimum wind speed were considered in order to make a complete assessment of wind energy potential. These can be obtained from k and c parameters. The most probable wind speed (V_{mp}) represents the most frequent wind speed (m s^{-1}) of a given probability distribution. This can be calculated as follows (Chang 2011; Mostafaeipour et al. 2011):

$$V_{mp} = c\left(1 - \frac{1}{k}\right)^{\frac{1}{k}}. \tag{6}$$

The optimum wind speed (V_{op}) represents the wind speed, which carries the maximum amount of wind energy. It is expressed as (Jamil, Parsa, and Majidi 1995)

$$V_{op} = c\left(1 + \frac{2}{k}\right)^{\frac{1}{k}}. \tag{7}$$

Wind power density and wind energy

The power of the wind flowing through a sweep area of a wind turbine is proportional to the cube of wind speed. This is given by (Ucar and Balo 2009)

$$P_v = \frac{1}{2}\rho A V^3, \tag{8}$$

where P_v is the wind power (W), ρ is the air density (kg m^{-3}), and A is the sweep area of the rotor blades (m^2). The wind power density based on the Weibull probability density function can be expressed in the following way (Ohunakin 2011):

$$p_v = \frac{P_v}{A} = \frac{1}{2}\rho c^3 \Gamma\left(1 + \frac{3}{k}\right), \tag{9}$$

where p_v is the wind power density (W m^{-2}) and Γ is the Gamma function. According to Manwell, McGowa, and Rogers (2002), values of $p_v < 100$, ~400, and > 700 W m^{-2} are defined as poor, good, and great, respectively. Wind energy density (E) for a desired duration (T) can be calculated as

$$E = \frac{1}{2}\rho c^3 \Gamma\left(1 + \frac{3}{k}\right) T. \tag{10}$$

Wind turbine energy output and capacity factor

The energy generated by a wind turbine for a particular time period was calculated using Weibull distribution and chronological data methods. The former method ($Ewt_{(W)}$), which was applied in the further calculations, can be used with acceptable accuracy for wind energy prediction (Kitaneh, Alsamamra, and Aljunaidi 2012) and it is given by the following expression (adapted from Chang and Tu 2007):

$$\begin{aligned} Ewt_{(W)} &= T \int_{V_i}^{V_0} P_{wt}(V) f(V) dv \\ &= T \int_{Vi}^{Vo} P_{wt}(V) \frac{k}{c}\left(\frac{V}{c}\right)^{k-1} \exp\left[-\left(\frac{V}{c}\right)^{k}\right] V, \end{aligned} \tag{11}$$

where $P_{wt}(V)$ is the output power at a given speed for a wind turbine, V_i is the cut-in wind speed (m s^{-1}), and V_0 is the cut-out wind speed (m s^{-1}). The chronological data method ($Ewt_{(CD)}$) is (Chang and Tu 2007)

$$Ewt_{(CD)} = \sum_{i=1}^{n} P_{wt}(V)\Delta t_i, \tag{12}$$

where Δt_i is the time-series interval.

The capacity factor (C_f) of a wind turbine represents the fraction of the total energy generated over a period ($Ewt_{(W)}$) divided by the energy of the turbine operating at the rated power (P_r) over the entire period (T) ($E_r = P_r{*}T$). The following equation is used:

$$C_f = \frac{Ewt_w}{E_r}. \tag{13}$$

Table 2. Technical description of the considered wind turbine models.

Wind turbine model	Location	Hub height (m)	Swept blade area (m^2)	Cut-in wind speed (m s^{-1})	Rated wind speed (m s^{-1})	Cut-out wind speed (m s^{-1})	Rated power (kW)
IVS-4500	Onshore	10	64	4.0	13.0	40	4.5
Windflow 500	Onshore	30	866	5.5	13.7	30	500
Vestas V39	Offshore	40	1195	4.5	16.0	50	500
SURU54 177-750	Onshore	60	2546	3.0	11.5	25	750
Vestas 90-3.0 MW	Offshore	+60	6362	3.5	15.0	25	3000

According to Milbrandt and Mann (2007), a reasonable capacity factor is 0.25 to 0.30; a very good capacity factor is 0.40. The technical description of the commercial wind turbines considered in this article is summarized in Table 2.

Economic Analysis

It is essential to make an accurate estimation of all costs throughout a wind turbine life-cycle. The cost of electricity produced for a given turbine can be calculated from the present value cost (PVC), expressed as follows (modified from Realpe, Diazgranados, and Acevedo Morantes 2012):

$$PVC = I + C_{om}\left[\frac{1+i}{r-i}\right]\left[1-\left(\frac{1+i}{1+r}\right)\right] - S\left(\frac{1+i}{1+r}\right)^{t}, i > , \tag{14}$$

where I is the investment cost given by the wind turbine price plus its 20%. Wind turbine prices depend on the turbine size (kW), but they vary according to manufacturers. In this work, the website http://www.windustry.org was consulted in order to obtain information on wind turbine prices. Operation, maintenance, and repair costs (C_{om}) were considered to be 25% of the annual cost of the turbine (machine price/lifetime) (e.g., Bagiorgas et al. 2007; Ahmed Shata 2010; Realpe, Diazgranados, and Acevedo Morantes 2012).The interest rate (r) and inflation rate (i) were taken to be 13% and 10%, respectively. Scrap value (S) was taken to be 10% of the turbine price, and the turbine lifetime (t) was assumed to be 20 years.

The payback period for each wind turbine can be obtained once the PVC has been estimated and the local electricity tariff has been fixed. The electricity cost is estimated dividing the PVC by the annual amount of energy produced by a wind turbine over its lifetime.

Results and discussion

Wind sites assessment

The two-dimensional plots in Figure 2 show the histograms of the recorded wind speed and direction data for the study sites at 10 m height. The study region is mainly controlled by the latitudinal movement of the South Atlantic (Subtropical) anticyclone high-pressure system and by the passage of cold fronts. As a result, the prevalent wind direction in all sites is from the NW (Figure 2). In temperate regions, the changes in the wind direction are usually expected up to 180° (Mirhosseini, Sharifi, and Sedaghat 2011) as can be clearly seen in Figure 2(a) and (b). In addition, the coastal zone of Buenos Aires province is subject to short-term meteorological phenomena locally known as *Sudestada*, which is characterized by strong southeastern winds.

It can be concluded that the wind regime is more homogenous at sites located in the open bay (i.e., PC, MH, and OT) (Figure 2(c)–(e)) than at the two remaining sites (Figure 2(a)–(b)). Particularly, the sites located in the open bay showed a similar pattern, despite differences in speed values. For instance, the mean wind speed blowing from WNW to NNW ranged between 2 and 6 m s^{-1} in onshore sites (i.e., PC and MH) and between 3 and 12 m s^{-1} in the offshore site.

Monthly mean wind speed was plotted at 10 and 60 m height for all sites (Figure 3). The wind speed of the study sites presented a similar temporal pattern. In general terms, wind speed reaches its highest values during the period October to February, while the lowest values occur during autumn and winter (Figure 3). The results suggest that, in comparison to the onshore sites, the offshore site showed higher values of wind speed in all months. The latter is especially observable at 10 m height, where the wind speed in that site is not obviously affected by any surrounding roughness elements. Monthly mean wind speed at 10 m height varied between 3.8 and 6.8 m s^{-1} and between 6 and 8.6 m s^{-1} in onshore and offshore sites, respectively. Monthly mean wind speed extrapolated to a height of 60 m ranged between 6.3 and 9.2 m s^{-1} and between 7.2 and 10.3 m s^{-1} in onshore and offshore sites, respectively.

Turbulence intensity for all sites at 30 m height was plotted as function of average wind speed from 4 m s^{-1} (Figure 4). This threshold is due to the fact that the cut-in wind speed required by a wind turbine to start up is usually between 3 and 5 m s^{-1}. Within the study period, the turbulence reached mean values of 0.16, 0.17, 0.21, 0.24, and 0.09 in GC, VM, PC, MH, and OT sites, respectively. According to the literature, turbulence levels over oceans are typically lower than over land (Barthelmie et al. 2003, 2007). Coincident with this, it can be seen that the onshore sites are characterized by a moderate level of turbulence (Figure 4(a)–(d)) whereas the offshore site exhibited a low level of turbulence (Figure 4(e)). Therefore, these conditions are favorable for the efficiency of wind turbines.

On the basis of the wind speed data recorded, the Weibull probability density function was determined. Table 3 shows the results obtained from the calculation of the monthly shape and scale parameters for each site at 10, 30, and 60 m height. The Weibull distribution may vary from site to site, both in shape and scale parameters (Mostafaeipour et al. 2011) as in this case.

The k parameter exhibits a small inter-monthly variability in all sites, characterized by discontinuous peaks, which are

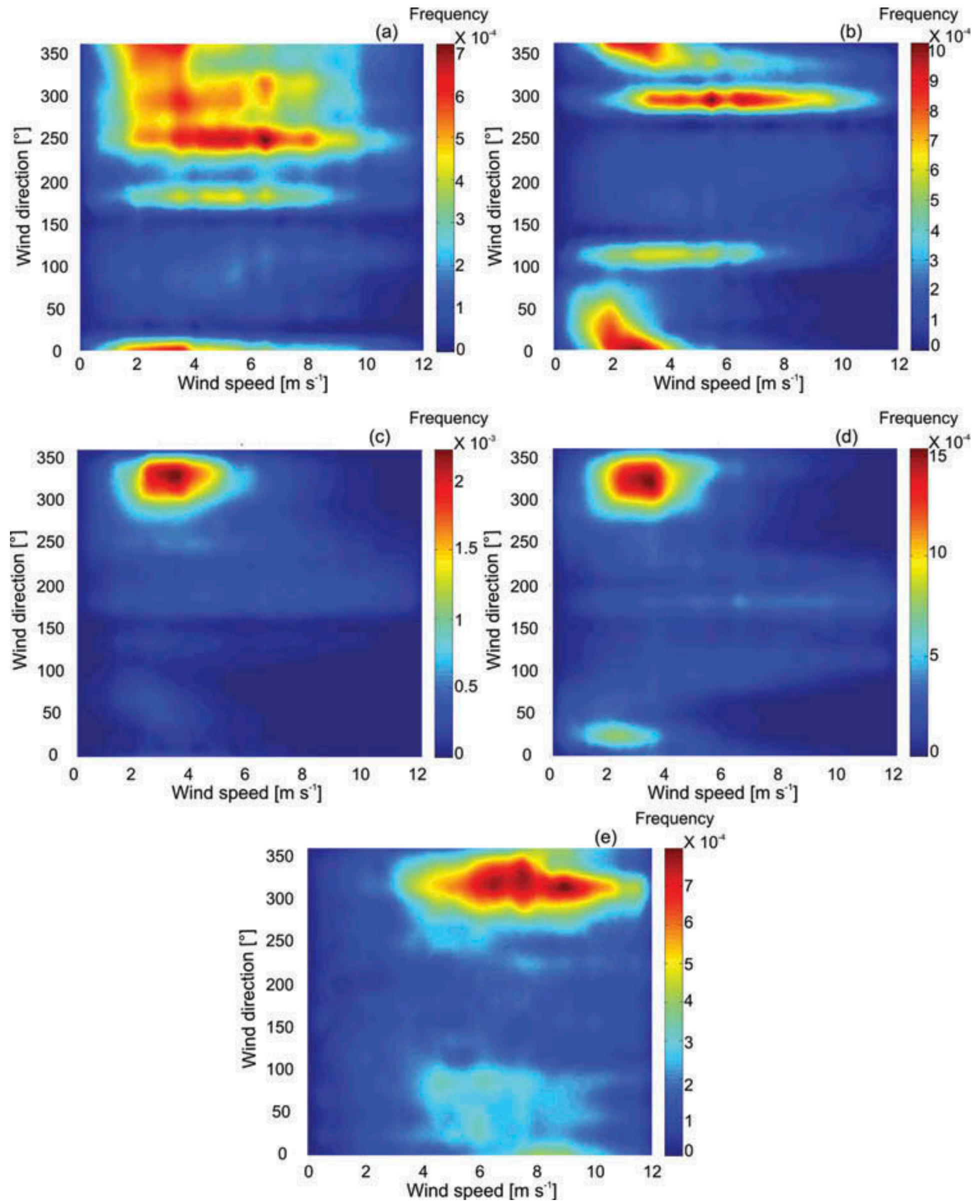

Figure 2. Mean wind speed and direction at 10 m height for GC (a), VM (b), PC (c), MH (d), and OT (e) sites.

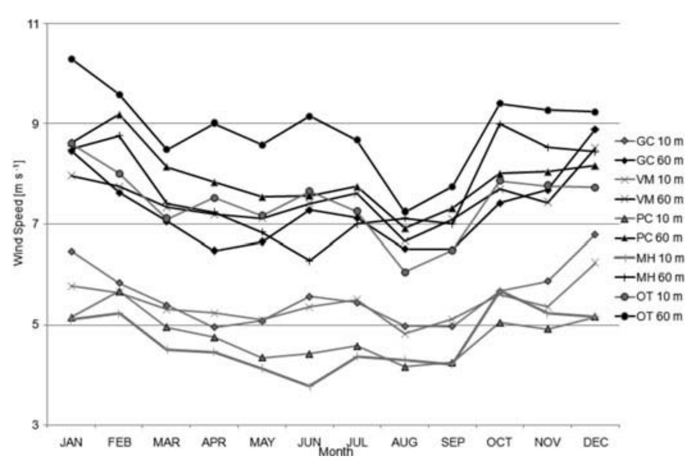

Figure 3. Monthly mean wind speed at 10 and 60 m height for all sites.

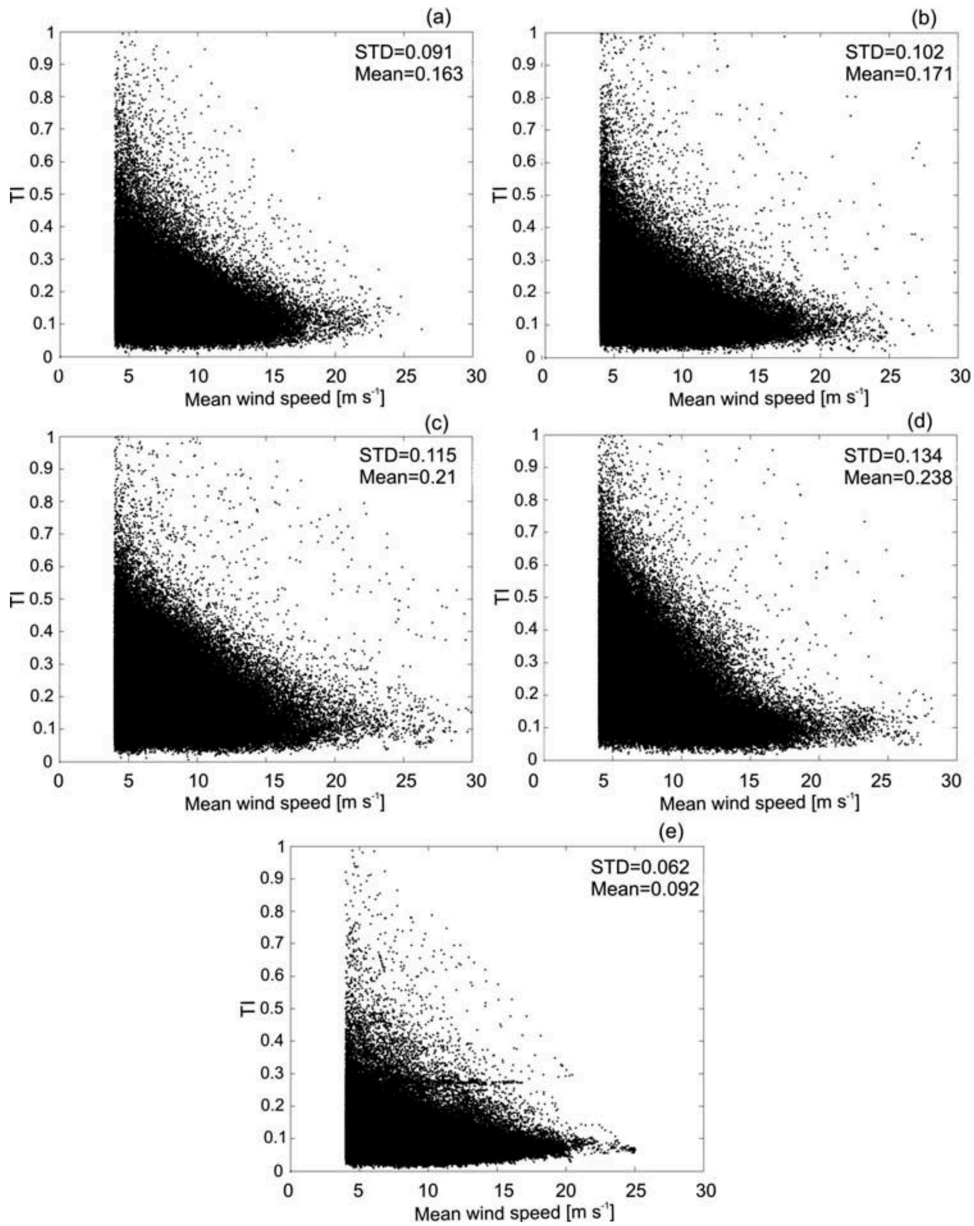

Figure 4. Variation of turbulence intensity as a function of mean wind speed at a heigth of 30 m, for GC (a), VM (b), PC (c), MH (d), and OT (e) sites. Threshold wind speed = 4 m s^{-1}.

slightly more visible from October to January. Considering onshore sites at an intermediate height (i.e., 30 m), the monthly values of k varied from 1.62 to 2.18 in GC, from 1.51 to 1.71 in VM, from 1.64 to 1.94 in PC, and from 1.56 to 1.79 in MH. The offshore site varied from 2.1 to 2.67. At the same height, the sites showed an annual value of 1.86, 1.68, 1.81, 1.68, and 2.4 for GC, VM, PC, MH, and OT, respectively (Table 3). The shape parameter distribution shows a trend toward lower speeds in onshore sites, whereas in the offshore site, it indicates a trend toward higher speeds.

As regards the c parameter, and taking into account it is dependent on both the shape parameter and the observed wind speed (Olaofe and Folly 2013), a similar pattern to k parameter was found (Table 3). At an intermediate height, the monthly values of c varied from 6.5 to 9.1 m s^{-1} in GC, from 6.6 to 8.5 m s^{-1} in VM, from 6.3 to 8.4 m s^{-1} in PC, from 5.9 to 8.4 m s^{-1} in MH, and from 7.6 to 10.8 m s^{-1} in OT. The annual value was 7.4, 7.4, 7.3, 7.1, and 9.3 m s^{-1} for GC, VM, PC, MH, and OT, respectively.

Based on k and c parameters, the most probable and optimum wind speed were obtained for all sites at 10, 30, and 60 m height (Table 4). Inter-monthly variability indicates a similar trend to those above-mentioned. In all cases, both the most probable and optimum wind speed increase with height. Within the study period, the highest most probable wind speeds at each site, for example, at a height of 30 m, were 6.5 m s^{-1} (December), 4.9 m s^{-1} (July), 5.6 m s^{-1} (February), 4.9 m s^{-1} (January, October), and 9 m s^{-1} (January) for GC, VM, PC, MH, and OT, respectively (Table 4). Figure 5 shows the frequency of occurrence

Table 3. Monthly and annual values of weibull parameters (*k* and *c*) for all sites at different heights.

Month	Hub height		GC	VM	PC	MH	OT
JAN	10	*k*	2.180	1.624	1.707	1.636	2.607
		c	7.217	6.374	5.945	5.856	9.714
	30	*k*	2.180	1.661	1.839	1.742	2.607
		c	8.509	7.769	8.147	7.996	10.842
	60	*k*	2.180	1.684	1.917	1.801	2.607
		c	9.442	8.805	9.964	9.753	11.620
FEB	10	*k*	1.942	1.668	1.710	1.628	2.098
		c	6.501	6.203	6.210	5.549	8.704
	30	*k*	1.942	1.708	1.866	1.717	2.098
		c	7.665	7.556	8.378	7.685	9.715
	60	*k*	1.942	1.732	1.965	1.763	2.098
		c	8.505	8.560	10.147	9.459	10.412
MAR	10	*k*	1.795	1.663	1.540	1.544	2.318
		c	6.139	5.966	5.551	5.045	7.981
	30	*k*	1.795	1.699	1.638	1.663	2.318
		c	7.239	7.279	7.552	6.854	8.908
	60	*k*	1.795	1.721	1.697	1.738	2.318
		c	8.032	8.254	9.188	8.332	9.547
APR	10	*k*	1.851	1.658	1.538	1.572	2.241
		c	5.572	5.980	5.457	5.106	8.506
	30	*k*	1.851	1.687	1.644	1.675	2.241
		c	6.570	7.267	7.410	6.875	9.494
	60	*k*	1.851	1.704	1.710	1.739	2.241
		c	7.290	8.220	9.003	8.306	10.176
MAY	10	*k*	1.688	1.573	1.686	1.537	2.579
		c	5.577	5.499	4.700	4.438	8.165
	30	*k*	1.688	1.597	1.771	1.630	2.579
		c	6.576	6.760	6.619	6.086	9.113
	60	*k*	1.688	1.610	1.816	1.684	2.579
		c	7.297	7.704	8.231	7.440	9.767
JUN	10	*k*	1.840	1.611	1.722	1.627	2.443
		c	6.270	6.135	5.047	4.299	8.465
	30	*k*	1.840	1.633	1.818	1.716	2.443
		c	7.393	7.492	7.021	5.878	9.448
	60	*k*	1.840	1.645	1.871	1.765	2.443
		c	8.203	8.500	8.661	7.173	10.127
JUL	10	*k*	1.802	1.831	1.847	1.462	2.378
		c	6.199	6.086	5.156	4.914	8.175
	30	*k*	1.802	1.847	1.902	1.556	2.378
		c	7.309	7.433	7.112	6.583	9.125
	60	*k*	1.802	1.855	1.923	1.617	2.378
		c	8.110	8.436	8.732	7.926	9.779
AUG	10	*k*	1.615	1.649	1.590	1.573	2.413
		c	5.566	5.401	4.600	4.756	6.775
	30	*k*	1.615	1.665	1.670	1.668	2.413
		c	6.563	6.590	6.283	6.490	7.561
	60	*k*	1.615	1.674	1.712	1.719	2.413
		c	7.282	7.475	7.668	7.914	8.104
SEP	10	*k*	1.734	1.668	1.782	1.641	2.202
		c	5.557	5.655	4.754	4.816	7.390
	30	*k*	1.734	1.692	1.862	1.701	2.202
		c	6.553	6.925	6.635	6.571	8.248
	60	*k*	1.734	1.706	1.897	1.722	2.202
		c	7.271	7.872	8.208	8.013	8.840
OCT	10	*k*	1.892	1.649	1.814	1.565	2.593
		c	6.462	6.380	5.740	6.283	8.849
	30	*k*	1.892	1.664	1.936	1.681	2.593
		c	7.620	7.751	7.624	8.383	9.876
	60	*k*	1.892	1.671	2.004	1.754	2.593
		c	8.455	8.765	9.141	10.076	10.585
NOV	10	*k*	1.947	1.715	1.783	1.513	2.666
		c	6.527	6.050	5.605	5.870	8.710
	30	*k*	1.947	1.746	1.880	1.604	2.666
		c	7.696	7.386	7.546	7.932	9.722
	60	*k*	1.947	1.765	1.930	1.658	2.666
		c	8.539	8.380	9.123	9.610	10.420
DEC	10	*k*	2.010	1.500	1.807	1.698	2.234
		c	7.752	7.036	5.770	5.653	8.891
	30	*k*	2.010	1.513	1.920	1.785	2.234
		c	9.141	8.543	7.658	7.668	9.924
	60	*k*	2.010	1.520	1.986	1.826	2.234
		c	10.142	9.658	9.173	9.315	10.636
ANUAL	10	*k*	1.858	1.651	1.711	1.583	2.398
		c	6.278	6.064	5.378	5.215	8.360
	30	*k*	1.858	1.676	1.812	1.678	2.398
		c	7.403	7.396	7.332	7.083	9.331
	60	*k*	1.858	1.691	1.869	1.732	2.398
		c	8.214	8.386	8.937	8.610	10.001

Table 4. Most probable and optimum wind speed for all sites at different heights.

		Most probable wind speed (m s^{-1})					Optimum wind speed (m s^{-1})				
Month	Hub height	GC	VM	PC	MH	OT	GC	VM	PC	MH	OT
JAN	10	5.45	3.54	3.55	3.29	8.07	9.73	10.45	9.36	9.54	12.09
	30	6.42	4.46	5.32	4.90	9.01	11.47	12.50	12.16	12.40	13.49
	60	7.12	5.16	6.78	6.22	9.65	12.73	14.02	14.46	14.77	14.46
FEB	10	4.48	3.58	3.71	3.09	6.39	9.36	9.95	9.77	9.08	11.98
	30	5.28	4.51	5.55	4.62	7.14	11.04	11.90	12.38	12.05	13.37
	60	5.86	5.21	7.07	5.88	7.65	12.25	13.33	14.50	14.54	14.33
MAR	10	3.90	3.43	2.81	2.57	6.26	9.32	9.59	9.53	8.64	10.44
	30	4.60	4.32	4.25	3.94	6.98	10.99	11.51	12.29	11.02	11.65
	60	5.10	4.98	5.44	5.09	7.48	12.19	12.92	14.54	12.95	12.49
APR	10	3.66	3.42	2.76	2.68	6.53	8.28	9.64	9.38	8.61	11.31
	30	4.32	4.27	4.19	4.00	7.29	9.76	11.55	12.02	10.99	12.62
	60	4.79	4.89	5.38	5.08	7.82	10.83	12.96	14.16	12.90	13.53
MAY	10	3.28	2.89	2.76	2.24	6.75	8.86	9.26	7.47	7.63	10.20
	30	3.86	3.65	4.14	3.40	7.53	10.45	11.24	10.14	9.95	11.39
	60	9.00	4.22	5.30	4.36	8.08	11.59	12.72	12.39	11.84	12.20
JUN	10	4.09	3.36	3.05	2.39	6.82	9.35	10.13	7.90	7.04	10.81
	30	4.83	4.19	4.52	3.53	7.62	11.03	12.23	10.56	9.22	12.07
	60	5.36	4.81	5.76	4.47	8.16	12.24	13.79	12.77	11.02	12.94
JUL	10	3.96	3.95	3.38	2.23	6.50	9.38	9.11	7.67	8.86	10.57
	30	4.66	4.87	4.80	3.40	7.25	11.06	11.06	10.38	11.20	11.79
	60	5.18	5.56	5.96	4.37	7.77	12.27	12.51	12.65	13.04	12.64
AUG	10	3.06	3.07	2.47	2.50	5.43	9.17	8.74	7.68	8.01	8.70
	30	3.61	3.80	3.64	3.75	6.06	10.81	10.58	10.07	10.41	9.71
	60	4.01	4.34	4.59	4.77	6.49	11.99	11.95	12.05	12.40	10.41
SEP	10	3.38	3.27	2.99	2.72	5.61	8.65	9.07	7.25	7.83	9.91
	30	3.99	4.08	4.39	3.90	6.27	10.20	10.98	9.82	10.38	11.06
	60	4.43	4.69	5.53	4.84	6.72	11.32	12.40	12.00	12.54	11.85
OCT	10	4.34	3.62	3.69	3.28	7.33	9.46	10.33	8.65	10.63	11.03
	30	5.12	4.46	5.24	4.90	8.18	11.16	12.46	11.00	13.36	12.31
	60	5.68	5.08	6.47	6.23	8.77	12.38	14.04	12.91	15.55	13.20
NOV	10	4.51	3.63	3.53	2.87	7.30	9.38	9.50	8.55	10.24	10.74
	30	5.31	4.54	5.04	4.31	8.15	11.06	11.44	11.09	13.14	11.99
	60	5.90	5.22	6.25	5.50	8.74	12.28	12.87	13.19	15.49	12.85
DEC	10	5.50	3.38	3.69	3.35	6.82	10.93	12.38	8.72	8.94	11.84
	30	6.49	4.18	5.22	4.84	7.61	12.89	14.91	11.11	11.68	13.21
	60	7.20	4.77	6.45	6.03	8.15	14.30	16.78	13.03	13.97	14.16

histograms of the wind speed at 30 m height and the Weibull curve fit for the month of the year with the highest value of most probable wind speed at each site. The most probable wind speed represented the 8%–9% of the distribution in all sites (Figure 5). The optimum wind speeds carrying maximum energy at 30 m height were 12.9 m s^{-1} (December), 14.9 m s^{-1} (December), 12.4 m s^{-1} (February), 13.4 m s^{-1} (October), and 13.5 m s^{-1} (January) for GC, VM, PC, MH, and OT sites, respectively (Table 4).

The monthly wind power density based on the Weibull probability density function was plotted for the selected sites at different heights (Figure 6). Along the year, the sites displayed strong monthly differences, with peaks in summer months. The annual amounts of power density at 30 m height decreased in the following order: 6898 W m^{-2} (OT), 5056 W m^{-2} (VM), 4471 W m^{-2} (MH), 4411 W m^{-2} (PC), and 4386 W m^{-2} (GC). Unlike this, the annual power density at 60 m height was: 8463 W m^{-2} (OT), 7622 W m^{-2} (PC), 7612 W m^{-2} (MH), 7245 W m^{-2} (VM), and 5971 W m^{-2} (GC).

Concerning wind power categorization and following Manwell, McGowa, and Rogers (2002), it was found that the onshore sites have a relatively good situation with respect to power density from a height of 30 m, while below that level, power density is poor in almost every month (Figure 6(a)–(d)). In contrast, at a height of 10 m, the offshore site achieved a good level of power density in all months, except August (Figure 6(e)). At higher altitudes (i.e., 60 m) power density is greater during several months, especially marked in the offshore site (Figure 6).

Energy production and cost assessment

Annual energy output was estimated for the selected wind turbine models (Table 2) in all sites using Equations (11) and (12) corresponding to Weibull and chronological data methods, respectively (Figure 7). The annual energy values obtained from Weibull method were higher than those obtained from chronological data method for all onshore sites. Unlike this, in the offshore site, the energy values obtained from chronological method were slightly higher than the other method.

The Vestas V90 offshore wind turbine model generated the highest quantity of annual energy output, reaching 7135 and 7185 MWh per year by using Weibull and chronological data methods, respectively (Figure 7). Results concerning the medium-scale wind turbines of 500 (Windflow 500) and 750 kW (SURU54 177-750) operating in onshore sites showed that the highest performance occurred in VM and PC sites, respectively (Figure 7). The annual energy output of the former wind turbine reached 828 and 657 MWh per year in VM by using probabilistic and chronological methods, respectively, while the SURU54 177-750 wind turbine reached 2476 (probabilistic method) and 2256 MWh per year (chronological method) in PC. The onshore and offshore wind turbines with a rated power of 500 kW (i.e.,

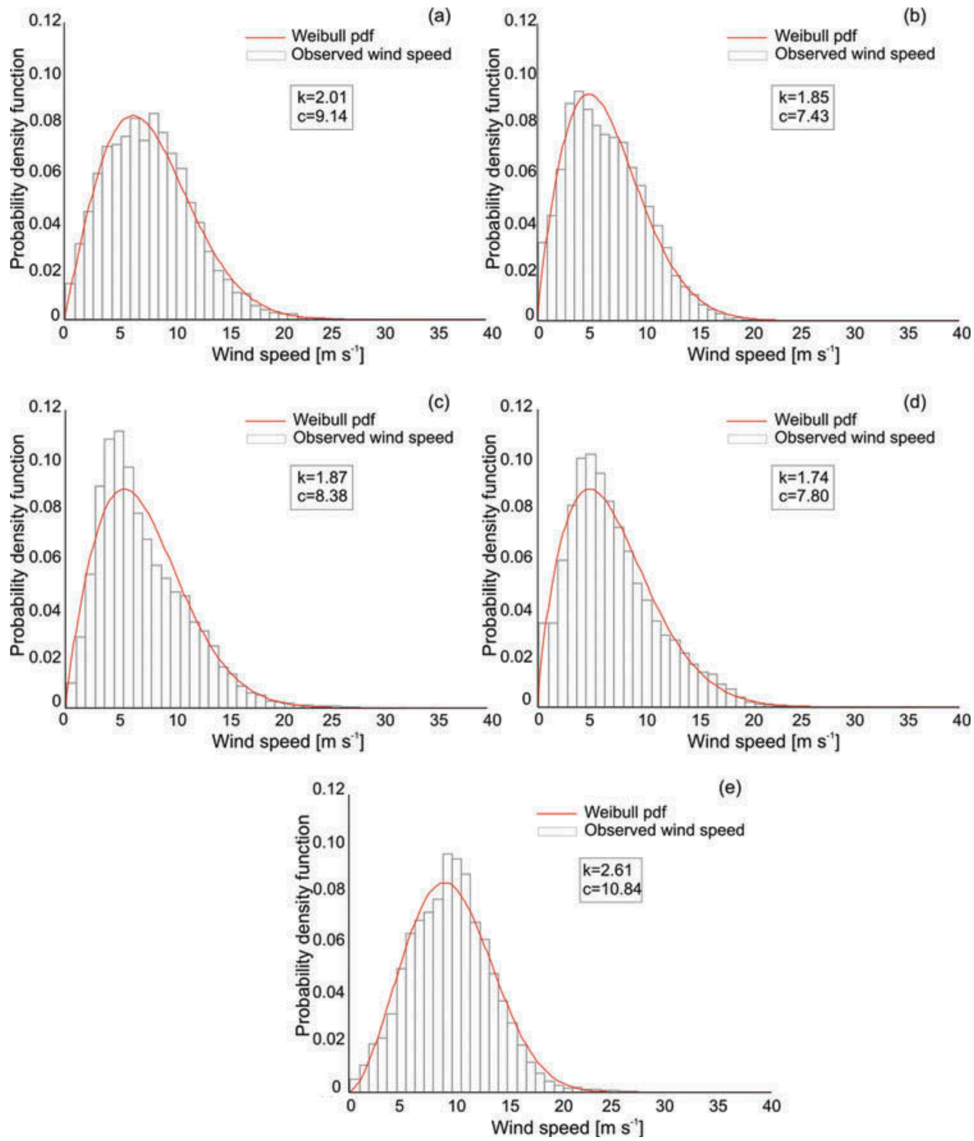

Figure 5. Histograms of the observed wind speed at 30 m height and the Weibull curve fit for the month with the highest value of most probable wind speed for GC (a), VM (b), PC (c), MH (d), and OT (e) sites.

Windflow 500 and Vestas V39) had a relatively similar performance in their respective zones (Figure 7). But it should be pointed out that the offshore wind turbine can operate for large wind speed intervals because its hub height is located at a greater height than the previous one. In the case of the small-scale wind turbine (i.e., IVS-4.5kW) operating in onshore sites, it ranged between 3.1 MWh per year (chronological method) in PC and 4.9 MWh per year (Weibull method) in VM (Figure 7).

The monthly capacity factor estimated using Equations (11) and (13) and the number of working days per month of the selected wind turbines are shown in Table 5. The highest values of both monthly capacity factor and number of working days occur in the summer months. In onshore sites, the best capacity factor reached 0.46, being obtained by SURU54 177-750 kW wind turbine model in GC (December; 257 MWh per month) and in PC (February; 232 MWh per month) (Table 5).

The most powerful wind turbine considered in this article (i.e., Vestas 90-3,000 kW) showed an annual capacity factor of 0.27 (i.e., 7,135 MWh per year) with 333.7 working days per year, favored by the lower cut-in wind speed. According to the class described by Milbrandt and Mann (2007), this offshore wind turbine had a good performance. The annual capacity factor corresponding to the onshore wind turbine operating at 60 m height (i.e., SURU54 177-750 kW) was 0.33, 0.34, 0.38, and 0.35 for GC, VM, PC, and MH, respectively. Therefore, the capacity proves to be good for GC and VM and very good for PC and MH sites. The annual capacity factor belonging to the wind turbine of 500 kW in both onshore and offshore regions was 0.17, 0.19, 0.19, 0.18, and 0.20 for GC, VM, PC, MH, and OT, respectively, displaying a regular performance. Finally, concerning the onshore IVS-4.5 kW wind turbine model, it exhibits annual capacity factor values of 0.08 to 0.12, which indicate a poor performance.

The wind energy possibility is determined through economic analysis. The cost per kWh of wind energy produced was plotted for all sites using different types of turbines

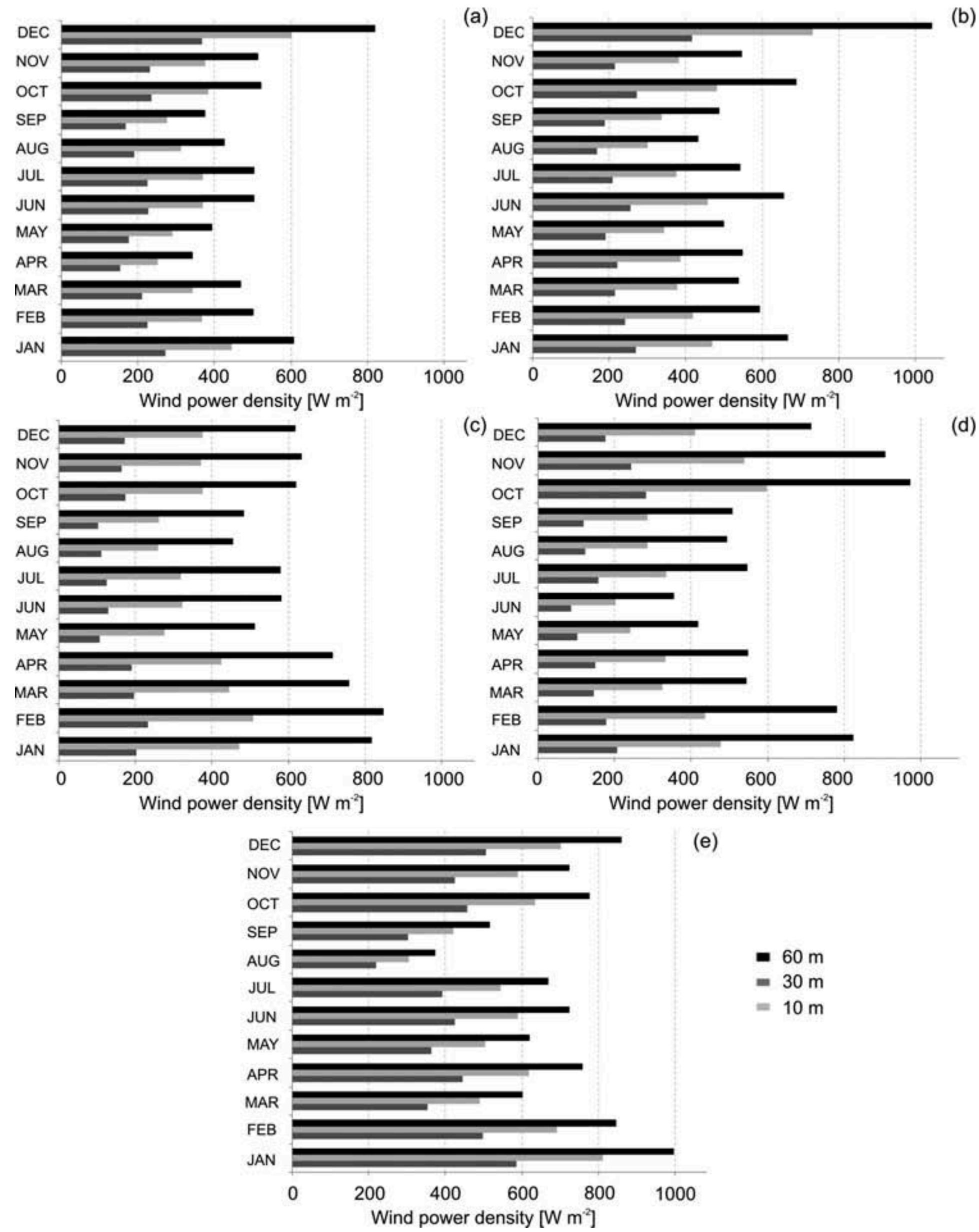

Figure 6. Monthly wind power density at different height for GC (a), VM (b), PC (c), MH (d), and OT (e) sites.

(Figure 8). Electricity costs decreased with increasing rated power of the wind turbine in all cases, with the exception of the small turbine (i.e., IVS-4.5 kW) whose cost was positioned between the remaining onshore turbines, in GC and VM sites. Regarding the onshore wind turbines operating at 30 m height, electricity costs per kWh decreased in the following order: 0.0799 US$ (GC), 0.0767 US$ (MH), 0.0741 US$ (PC), and 0.0730 US$ (VM), whereas at 60 m the order was: 0.0506 US$ (GC), 0.0490 US$ (VM), 0.0471 US$ (MH), and 0.0439 US$ (PC). In the case of offshore wind turbines, electricity costs reached 0.0854 cents and 0.0256 cents US$ per kWh for Vestas V39 and Vestas V90, respectively.

In Argentina, energy production is partly subsidized by the federal government. However, subsidies will be gradually taken off from the electricity sector (Uasuf and Becker 2011). The two scenarios indicated strong differences (Figure 9). In all cases, the payback period considering the subsidized scenario doubled the number of years. Likewise, under this scenario, the payback period of all wind turbines exceeded the lifetime (assumed to be 20 years), with the exception of Vestas V90 wind turbine model, which reached a payback period of only 10.8 years. Concerning the remaining scenario (i.e., without subsidization) the payback period indicated that all turbines are economically viable. SURU54 177-750 kW wind turbine model showed the minimum payback period in onshore sites, with values ranging between 8.4 (PC) and 9.7 years (GC).

Conclusion

Wind energy potential is important for the social and economic development of the area, mainly in a context of high demand of energy consumption. The wind energy potential in coastal sites of Buenos Aires province (Argentina) was evaluated. Besides, the operational and economic

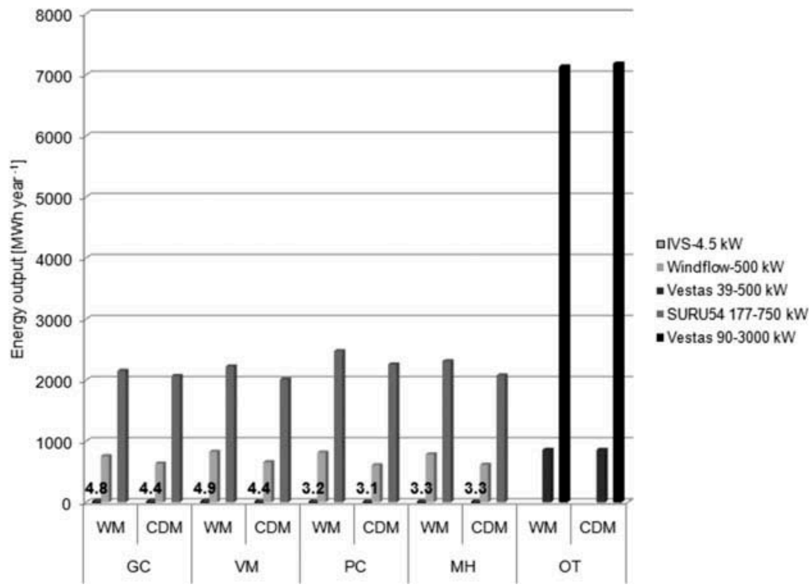

Figure 7. Annual energy output obtained with Weibull (WM) and chronological data (CDM) methods for GC (a), VM (b), PC (c), MH (d), and OT (e) sites.

Table 5. Capacity factor and number of working days of the different wind turbine models for the study sites.

Month	Hub height		GC	VM	PC	MH	OT
JAN	10	*Cf*	0.16	0.14	0.11	0.11	
		Nd	22.6	17.3	16.4	16.4	
	30	*Cf*	0.23	0.21	0.24	0.24	
		Nd	19.8	15.7	17.7	17.0	
	40	*Cf*					0.29
		Nd					28.5
	60	*Cf*	0.42	0.37	0.45	0.43	0.38
		Nd	27.5	25.6	27.8	26.9	29.5
FEB	10	*Cf*	0.13	0.13	0.13	0.09	
		Nd	18.3	16.1	15.5	14.1	
	30	*Cf*	0.18	0.20	0.25	0.22	
		Nd	16.4	14.4	16.1	14.7	
	40	*Cf*					0.23
		Nd					23.5
	60	*Cf*	0.35	0.35	0.46	0.41	0.30
		Nd	23.1	23.1	25.3	24.2	25.5
MAR	10	*Cf*	0.11	0.11	0.10	0.08	
		Nd	18.2	16.7	14.5	13.0	
	30	*Cf*	0.16	0.18	0.21	0.16	
		Nd	15.7	14.8	14.8	13.6	
	40	*Cf*					0.17
		Nd					25.4
	60	*Cf*	0.31	0.33	0.39	0.34	0.24
		Nd	24.7	25.0	26.6	26.0	27.9
APR	10	*Cf*	0.08	0.12	0.10	0.08	
		Nd	16.1	15.5	13.1	11.9	
	30	*Cf*	0.12	0.18	0.20	0.16	
		Nd	13.7	14	13.7	12.5	
	40	*Cf*					0.21
		Nd					24.9
	60	*Cf*	0.26	0.33	0.38	0.33	0.29
		Nd	23.6	23.6	25.7	25.1	27.3
MAY	10	*Cf*	0.09	0.10	0.05	0.05	
		Nd	16.4	15.7	12.6	11.4	
	30	*Cf*	0.13	0.16	0.15	0.12	
		Nd	14.2	14.2	13.6	11.7	
	40	*Cf*					0.17
		Nd					26.4
	60	*Cf*	0.26	0.3	0.33	0.28	0.25
		Nd	23.5	24.1	26.7	25.0	28.2
JUN	10	*Cf*	0.12	0.13	0.06	0.04	
		Nd	18.5	16.1	13.4	9.8	
	30	*Cf*	0.17	0.2	0.17	0.10	
		Nd	16.4	14.6	14	10.1	
	40	*Cf*					0.20
		Nd					25.8
	60	*Cf*	0.33	0.35	0.36	0.25	0.28
		Nd	24.2	23.9	25.7	23.9	27.9

(*Continued*)

Table 5. (Continued).

Month	Hub height		GC	VM	PC	MH	OT
JUL	10	*Cf*	0.12	0.11	0.06	0.08	
		Nd	18.2	18.5	15.1	12.0	
	30	*Cf*	0.17	0.18	0.17	0.16	
		Nd	15.4	16.7	15.7	13.02	
	40	*Cf*					0.18
		Nd					26.0
	60	*Cf*	0.32	0.34	0.36	0.31	0.26
		Nd	25.0	26.0	26.9	25.0	28.5
AUG	10	*Cf*	0.10	0.08	0.05	0.06	
		Nd	15.4	15.4	11.7	12.0	
	30	*Cf*	0.14	0.14	0.13	0.14	
		Nd	13.3	13.6	12	12.6	
	40	*Cf*					0.09
		Nd					24.5
	60	*Cf*	0.27	0.28	0.29	0.31	0.14
		Nd	22.8	24.1	25.4	25.4	27.3
SEP	10	*Cf*	0.09	0.1	0.05	0.06	
		Nd	15.8	16.4	12.2	11.9	
	30	*Cf*	0.13	0.16	0.14	0.15	
		Nd	13.7	14.3	13.1	13.2	
	40	*Cf*					0.14
		Nd					23.7
	60	*Cf*	0.26	0.31	0.33	0.31	0.20
		Nd	22.4	23.9	25.7	24.5	26.4
OCT	10	*Cf*	0.13	0.14	0.09	0.14	
		Nd	19.5	18.5	16.4	17.3	
	30	*Cf*	0.18	0.21	0.19	0.26	
		Nd	17.3	16.7	16.4	17.6	
	40	*Cf*					0.22
		Nd					27.6
	60	*Cf*	0.34	0.36	0.39	0.44	0.31
		Nd	25.4	25.0	26.9	26.9	29.1
NOV	10	*Cf*	0.13	0.12	0.09	0.12	
		Nd	20.0	17.0	15.5	15.5	
	30	*Cf*	0.18	0.18	0.19	0.24	
		Nd	17.6	15.2	15.5	16.8	
	40	*Cf*					0.21
		Nd					26.7
	60	*Cf*	0.35	0.34	0.39	0.41	0.29
		Nd	25.1	24.5	26.6	25.7	28.2
DEC	10	*Cf*	0.21	0.20	0.09	0.09	
		Nd	22.9	19.5	16.4	16.4	
	30	*Cf*	0.28	0.27	0.20	0.21	
		Nd	20.7	17.9	16.4	16.7	
	40	*Cf*					0.24
		Nd					26.0
	60	*Cf*	0.46	0.40	0.40	0.40	0.32
		Nd	27.2	25.4	27.2	26.9	27.9
ANNUAL	10	*Cf*	0.12	0.12	0.08	0.08	
		Nd	221.9	202.7	172.8	161.7	
	30	*Cf*	0.17	0.19	0.19	0.18	
		Nd	194.2	182.1	179	169.52	
	40	*Cf*					0.20
		Nd					309
	60	*Cf*	0.33	0.34	0.38	0.35	0.27
		Nd	294.5	294.2	316.5	305.5	333.7

performance of small- and medium-scale wind turbine models was assessed. In the offshore site, the speed is more pronounced (about 31%; V(OT) = 7.4 m s^{-1} at 10 m height) and less turbulent (about 53%; TI(OT) = 0.092) than in onshore sites. Based on the results of this study, the sites have enough potential for wind energy generation. It can be seen from Figure 6 that the onshore sites have a relatively good situation with respect to power density from a height of 30 m above ground. Unlike this, the offshore site achieved a good level of power density in almost every month from a height of 10 m. In addition, at higher altitudes (i.e., 60 m) the power density becomes greater for most of the months of the year in all study sites.

The Vestas V90 offshore wind turbine model showed the highest quantity of annual energy output, reaching about 7160 MWh per year. Results concerning the medium-scale wind turbines of 500 and 750 kW operating in onshore sites indicated that the highest performance occurred in VM (828 MWh per year—Weibull method) and in PC (2476 MWh per year—Weibull method) sites, respectively. The small-scale turbine (onshore model) showed values lower than 5 MWh per year in all sites. If investment decision were based on capacity factor,

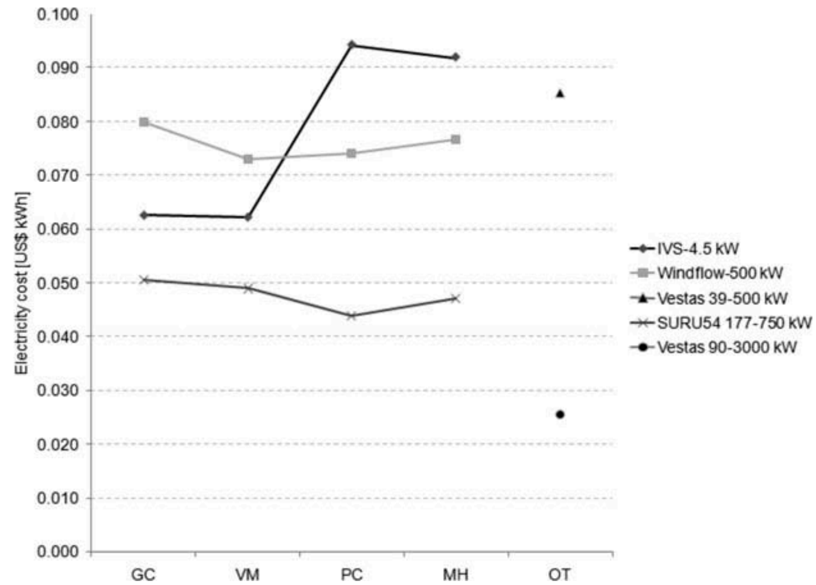

Figure 8. Cost of wind energy for all sites using the selected wind turbines.

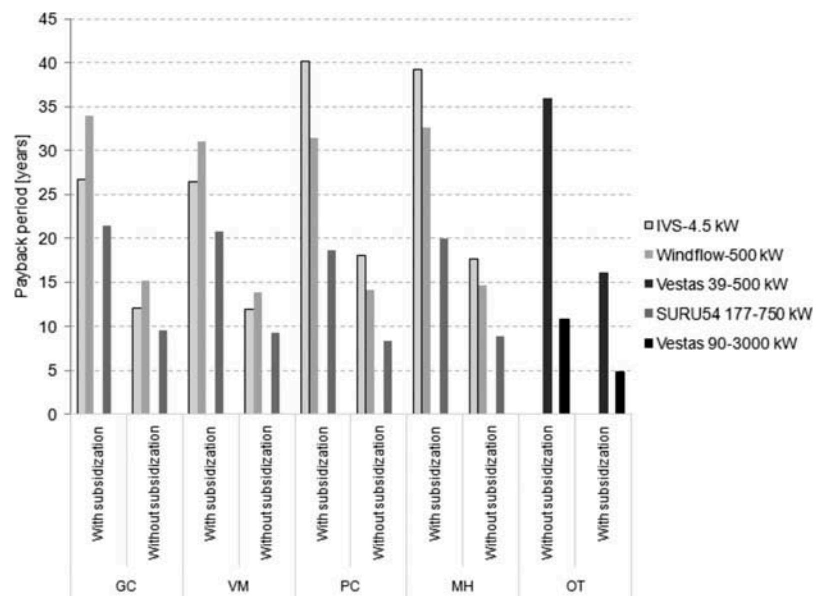

Figure 9. Payback period of the selected wind turbines for all sites, considering the two scenaries scenarios: with and without subsidization.

the SURU54 177-750 kW onshore model would be the best choice. In addition, under a non-subsidized scenario, this model proved to have the minimum payback period, with values ranging between 8.4 (PC) and 9.7 years (GC). The results derived from the present study encourage the construction of wind farms for electricity generation.

Acknowledgments

The authors are grateful to the CGPBB for providing the meteorological data of the oceanographic tower.

Funding

Financial support for this study was based on grants from the CONICET, Agencia Nacional de Promoción Científica y Tecnológica and the UNS.

References

Ahmed Shata, A. 2010. Wind energy as a potential generation source at Ras Benas, Egypt. *Renewable and Sustainable Energy Reviews* 14 (8):2167–73.

Andrawus, J. A., J. Watson, M. Kishk, and A. Adam. 2006. The selection of a suitable maintenance strategy for wind turbines. *Wind Engineering* 30(6):471–86.

Archer, C. L., and M. Z. Jacobson. 2003. Spatial and temporal distributions of U.S. winds and wind power at 80 m derived from measurements. *Journal of Geophysical Research: Atmospheres* 108(D9):10-1-10-20.

Ayodele, T. R., A. A. Jimoh, J. L. Munda, and J. T. Agee. 2012. Wind distribution and capacity factor estimation for wind turbines in the coastal region of South Africa. *Energy Conversion and Management* 64:614–25.

Bagiorgas, H. S., M. N. Assimakopoulos, D. Theoharopoulos, D. Matthopoulos, and G. K. Mihalakakou. 2007. Electricity generation using wind energy conversion systems in the area of Western Greece. *Energy Conversion and Management* 48(5):1640–55.

Bagiorgas, H. S., G. Mihalakakou, and D. Matthopoulos. 2008. A statistical analysis of wind speed distributions in the area of Western Greece. *International Journal of Green Energy* 5(1–2):120–37.

Barthelmie, R. J., L. Folkerts, F. T. Ormel, P. Sanderhoff, P. J. Eecen, O. Stobbe, and N. M. Nielsen. 2003. Offshore wind turbine wakes measured by sodar. *Journal of Atmospheric and Oceanic Technology* 20:466–77.

Barthelmie, R. J., S. T. Frandsen, M. N. Nielsen, S. C. Pryor, P. E. Rethore, and H. E. Jorgensen. 2007. Modelling and measurements of power losses and turbulence intensity in wind turbine wakes at Middelgrunden offshore wind farm. *Wind Energy* 10(6):517–28.

Bechrakis, D. A., and P. D. Sparis. 2000. Simulation of the wind speeds at different heights using artificial neural networks. *Wind Engineering* 24 (2):127–36.

Chang, T. J., and Y. L. Tu. 2007. Evaluation of monthly capacity factor of WECS using chronological and probabilistic wind speed data: A case study of Taiwan. *Renewable Energy* 32(12):1999–2010.

Chang, T. P. 2011. Estimation of wind energy potential using different probability density functions. *Applied Energy* 88(5):1848–56.

Diaf, S., and G. Notton. 2013. Evaluation of electricity generation and energy cost of wind energy conversion systems in southern Algeria. *Renewable and Sustainable Energy Reviews* 23:379–90.

Gualtieri, G., and G. Zappitelli. 2014. Investigating wind resource, turbulence intensity and gust factor on mountain locations in Southern Italy. *International Journal of Green Energy* 12(4):309–327.

Jamil, M., S. Parsa, and M. Majidi. 1995. Wind power statistics and an evaluation of wind energy density. *Renewable Energy* 6(5):623–8.

Janajreh, I., L. Su, and F. Alan. 2013. Wind energy assessment: Masdar City case study. *Renewable Energy* 52:8–15.

Karamanis, D. 2013. Wind energy resources analysis of Western Greece coast in terms of sustainable environmental indicators and towards their community-based exploitation in South-East Europe. *Journal of Renewable Sustainable Energy* 5:041801; doi:10.1063/1.4812654.

Kitaneh, R., H. Alsamamra, and A. Aljunaidi. 2012. Modeling of wind energy in some areas of Palestine. *Energy Conversion and Management* 62:64–9.

Labraga, J. C. 1994. Extreme winds in the Pampa del Castillo Plateau, Patagonia, Argentina, with reference to wind farm settlement. *Journal of Applied Meteorology* 33:85–95.

Manwell, J. F., J .G. McGowa, and A. L. Rogers. 2002. *Wind energy explained: Theory, design and application*. Amherst, USA: John Wiley & Sons.

Milbrandt, A., and M. Mann. 2007. *Potential for hydrogen production from key renewable resources in the United States*. Technical report NREL/TP-560–42773. Colorado, USA: National Renewable Energy Laboratory.

Mirhosseini, F., M. F. Sharifi, and A. Sedaghat. 2011. Assessing the wind energy potential locations in province of Semnan in Iran. *Renewable and Sustainable Energy Reviews* 15(1):449–59.

Molenaar, D. P. 2003. Cost-effective design and operation of variable speed wind turbines. Ph.D. thesis. The Netherlands: Delft University Press.

Morgan, E., M. Lackner, R. Vogel, and L. Baise. 2011. Probability distributions for offshore wind speeds. *Energy Conversion and Management* 52(1):15–26.

Mostafaeipour, A., A. Sedaghat, A. A. Dehghan-Niri, and V. Kalantar. 2011. Wind energy feasibility study for city of Shahrbabak in Iran. *Renewable and Sustainable Energy Reviews* 15(6):2545–56.

Ohunakin, O. S. 2011. Wind resource evaluation in six selected high altitude locations in Nigeria. *Renewable Energy* 36(12):3273–81.

Olaofe, Z. O., and K. A. Folly. 2013. Wind energy analysis based on turbine and developed site power curves: A case-study of Darling City. *Renewable Energy* 53:306–18.

Onea, F., and E. Rusu. 2013. An evaluation of the wind energy in the north-west of the black sea. *International Journal of Green Energy* 11 (5):465–87.

Palese, C., J. L. Lassig, M. G. Cogliati, and M. A. Bastanski. 2000. Wind regime and wind power in North Patagonia, Argentina. *Wind Engineering* 24(5):361–77.

Raichle, B. W., and W. R. Carson. 2009. Wind resource assessment of the Southern Appalachian Ridges in the Southeastern United States. *Renewable and Sustainable Energy Reviews* 13(5):1104–10.

Ramos, V., and G. Iglesias. 2014. Wind power viability on a small island. *International Journal of Green Energy* 11(7):741–60.

Realpe Jiménez, A., J. A. Diazgranados, and M. T. Acevedo Morantes. 2012. Electricity generation and wind potential assessment in regions of Colombia. *Dyna* 79(171):116–22.

Recalde, M. 2010. Wind power in Argentina: Policy instruments and economic feasibility. *International Journal of Hydrogen Energy* 35:5908–13.

Rehman, S., A. M. Mahbub Alam, J. P. Meyer, and L. M. Al-Hadhrami. 2012. Wind speed characteristics and resource assessment using Weibull parameters. *International Journal of Green Energy* 9(8):800–14.

Rodríguez, C. R., M. Riso, G. Jiménez Yob, R. Ottogalli, R. Santa Cruz, S. Aisa, G. Jeandrevin, and E. P. M. Leiva. 2010. Analysis of the potential for hydrogen production in the province of Córdoba, Argentina, from wind resources. *International Journal of Hydrogen Energy* 35:5952–6.

Sahin, B., and M. Bilgili. 2009. Wind characteristics and energy potential in Belen-Hatay, Turkey. *International Journal of Green Energy* 6 (2):157–72.

Stevens, M. J. M., and P. T. Smulders. 1979. The estimation of the parameters of the Weibull wind speed distribution for wind energy utilization purposes. *Wind Engineering* 3(2):132–45.

Tiang, T. L., and D. Ishak. 2012. Technical review of wind energy potential as small-scale power generation sources in Penang Island Malaysia. *Renewable and Sustainable Energy Reviews* 16(5):3034–42.

Türk Toğrul, I., and M. İmaş Kizi. 2008. Determination of wind energy potential and wind speed data in Bishkek, Kyrgyzstan. *International Journal of Green Energy* 5(3):157–73.

Uasuf, A., and G. Becker. 2011. Wood pellets production costs and energy consumption under different framework conditions in Northeast Argentina. *Biomass and Bioenergy* 35(3):1357–66.

Ucar, A., and F. Balo. 2009. Evaluation of wind energy potential and electricity generation at six locations in Turkey. *Applied Energy* 86 (10):1864–72.

Weisser, D. A. 2003. Wind energy analysis of Grenada: An estimation using the 'Weibull' density function. *Renewable Energy* 28:1803–12.

Zhang, J., S. Chowdhury, A. Messac, and L. Castillo. 2013. A multivariate and multimodal wind distribution model. *Renewable Energy* 51:436–47.